Three-Dimensional Reconstruction of Urogenital Tract From Visible Korean Human

JEAN-FRANÇOIS UHL,[1]* **JIN SEO PARK,**[2] **MIN SUK CHUNG,**[2] AND **VINCENT DELMAS**[1]

[1]Virtual Anatomy Unit, Department of Anatomy, University Paris V René Descartes, Paris, France

[2]Department of Anatomy, Ajou University School of Medicine, Suwon, South Korea

ABSTRACT

The three-dimensional (3D) modeling from anatomical images is revealed to be a remarkable learning tool in anatomy. This is particularly true for the pelvis area and the urogenital tract. The authors present here a 3D reconstruction of the male urogenital tract from the Visible Korean Human data. The segmentation of 440 anatomical images was arranged in a pile and processed by the SURFdriver software to build an interactive 3D model. Forty-two anatomical structures were reconstructed, including kidneys, ureters, urinary bladder (outer and inner boundaries), urethra, testes, epididymides, ducti deferens, seminal vesicles, prostate, rectum, anal canal, abdominal aorta, superior mesenteric artery, renal arteries, inferior vena cava, renal veins, lumbar vertebrae, intervertebral discs, sacrum, hip bones, femurs, and skin. Three-dimensional models of 42 anatomical structures can be individually and interactively manipulated. In addition, the use is able to control the transparency of the model. The aim of this computerized modeling is to present a learning tool for students and patients. In the near future, it could be the basis of new simulation tools for surgeon's training. Anat Rec Part A, 288A:893–899, 2006. © 2006 Wiley-Liss, Inc.

Key words: three-dimensional anatomy; Visible Korean Human; urogenital tract; virtual reality; 3D reconstruction; surgical simulation

The purpose of this research is to present an interactive three-dimensional (3D) model of the male urogenital tract. In order to achieve this purpose, the urogenital tract and adjacent anatomical structures were divided into its different parts on anatomical images of the Visible Korean Human (VKH) and then arranged in a pile to build a 3D vector-based model.

The understanding of the visiospatial aspects of anatomic structures is an important aspect of studying gross anatomy. The manipulation capabilities of a 3D model, such as translucent visualization, interactive rotation, translation, and scaling, facilitate fundamental learning experience that leads one to build 3D models in the mind, providing a validation of computer-assisted individual learning (Stephens et al., 2000).

Including 42 anatomical structures, from 440 segmented slices, this 3D model of the urogenital tract provides views of the structures from a new perspective and has the potential to improve understanding of the anatomical relationships of the pelvic region, particularly for students and patients.

History and Review of 3D Modeling of Anatomical Structures

Considerable effort was spent during the 1980s to develop algorithms capable of modeling surfaces. Two general approaches were developed: surface modeling and solid modeling.

Surface modeling reconstructs the object as a shell. Structures are digitized manually or automatically and tissue edges are represented as streams of coordinates or contours. A viewing space is defined by mapping a window and its world coordinate contents (x, y, and z) into the view port through a scaling function. The scaling function consists of the magnification factor and tissue thickness values. Geometric mapping algorithms are used to map coordinates for each contour to the subsequent contours on subsequent sections providing a wire-mesh model. The mesh model is rotated to a viewing angle and each surface tile is shaded according to the position of the light source and the viewer's eye.

Solid modeling represents the object as a discrete volume. A viewing space is defined as above and data input is made of voxels (pixel volumes). Voxels are stacked on (arranged in a pile) one another and the intensity is computed and applied to the stack. The solid model is rotated and the intensity values are applied to the image based on the position of the stack to the viewer's eye.

An alternate approach attempted to merge these two concepts was first described by Boissonnat (1988). Using this approach, volumes are constructed around contours using Delaunay and Voronoi diagrams.

Other Studies Using 3D Modeling of Male Urogenital Tract

For 10 years, the data set of Visible Human was used by several applications in the field of anatomy (Juanes et al., 2003). Some of these works concerned the urogenital tract. Brooks et al. (1998) presented the results of a 3D modeling of the male urogenital tract with 18 discrete anatomical structures, including the levator ani and stiated urethral sphincter. Venuti et al. (2004) also presented a 3D model of the visible human's urogenital tract visualized by Columbia University's in-house 3D Vesalius trademark Visualizer. By using this software, the 3D models depict the anatomy of the region in a realistic true-to-life color and texture. They can be used to create 3D anatomical scenes, with arbitrary complexity, where the component anatomical structures are displayed in correct 3D anatomical relationships. Moreover, a sequence of 3D scenes can be defined to simulate actual dissection. Structures can be added in a layered sequence from the bony framework to build from the inside-out or disassembled much like a true laboratory dissection from the outside-in.

MATERIALS AND METHODS

In this research, a 3D model of male urogenital tract was obtained by surface reconstruction from a 3D vectorial model. To obtain this 3D reconstructed model, precise segmented images were made on the basis of serially sectioned anatomical images of human body. The advantage of this data set, compared with computed tomographs or magnetic resonance images, is that all anatomical structures are clearly visible.

We decided to use the VKH data set, made at Ajou University School of Medicine, South Korea, for the following reasons.

First, the VKH included a male subject with precise body contour and position. The subject was neither fat nor lean (height, 164 cm; weight, 55 kg), so that an accurate 3D model including skin and bones could be obtained. Prior to serial sectioning, the bilateral hip joints of the
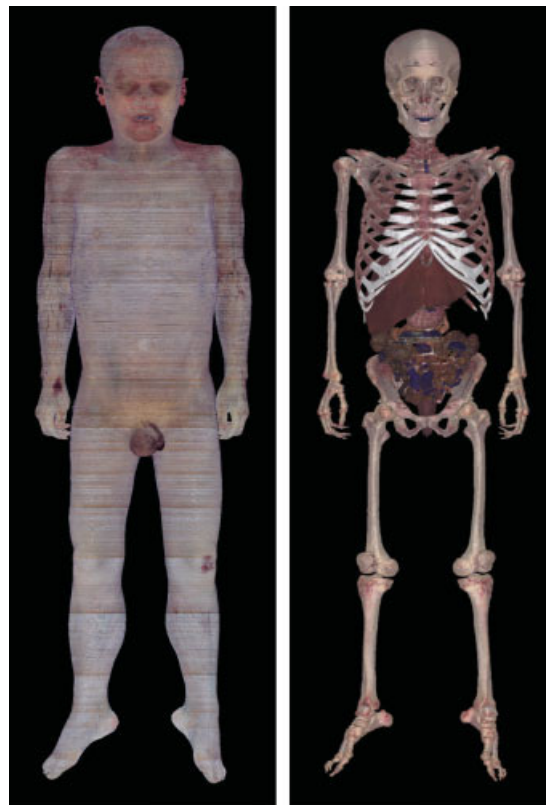

Fig. 1.   Three-dimensional model of whole body (left) and bones, internal organs (right) made of the VKH data.

subject were slightly abducted, so that the scrotum was not pressed by the bilateral thighs (Fig. 1) (Park et al., 2005a).

Second, the VKH included an intact urogenital tract in man of 33 years of age (Fig. 2) (Park et al., 2005a). The male subject of the VKH died of leukemia, which did not cause any pathological changes of the urogenital tract, including kidneys, ureters, urinary bladder, urethra, testes, and ducti deferens and adjacent anatomical structures such as bones (Fig. 2) (Park et al., 2005a). In contrast, the Visible Human Project used a male subject with a left orchiectomy (Spitzer et al., 1996).

Third, the VKH included high-quality anatomical images. The anatomical images of the VKH consisted of 0.2 mm-sized pixels (field of view, 600 mm $\times$ 400 mm; resolution, 3,040 $\times$ 2,008) with 24 bits color while those of the Visible Human Project had 0.33 mm-sized pixels (Spitzer et al., 1996). In the VKH, intervals of the anatomical images were 0.2 mm, so that every anatomical structure greater than 0.2 mm was identified without miss. In addition, neither fixative nor dye was perfused into the subject of the VKH to produce anatomical images with real color of living human body (Fig. 2) (Park et al., 2005a), while fixative or red dye was perfused into the subjects of the Visible Human Project and Chinese Visible Human (Spitzer et al., 1996; Zhang et al., 2003). Moreover, the anatomical images of the VKH were well aligned, which was verified on the coronal and sagittal planes of the anatomical images (Fig. 3) (Park et al., 2005a). On the
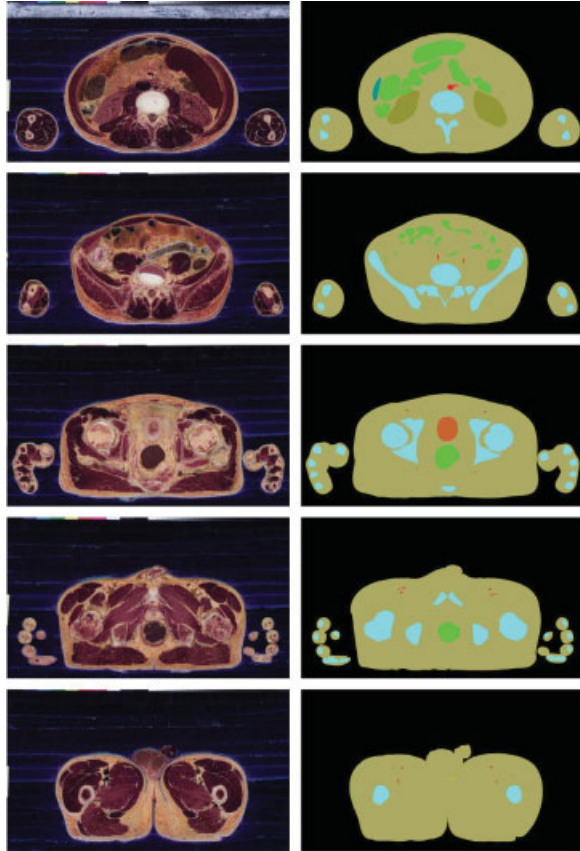
Fig. 2. Anatomical images (left column) and segmented images (right column) of the VKH from kidneys to testes.

basis of this high definition of anatomical images, segmented images of good quality could be produced.

Fourth, the VKH already included segmented images. On the anatomical images of the VKH, contours of basic anatomical structures such as kidneys, urinary bladder (outer boundary), abdominal aorta, renal arteries, lumbar vertebrae, sacrum, hip bones, femurs, and skin were drawn semiautomatically on the Adobe Photoshop version 7 software to make the basic segmented images. The drawing of the contours used the magic wand tool included in the photoshop software to facilitate the segmentation work. Correctness of the segmentation was verified by checking the coronal and sagittal planes of the segmented images (Fig. 3) (Park et al., 2005a, 2005b).

Thanks to the basic segmented images, in this research, we just needed to segment additional anatomical structures such as ureters, urinary bladder (inner boundary), urethra, testes, epididymides, ducti deferens, seminal vesicles, prostate, rectum, anal canal, superior mesenteric artery, inferior vena cava, renal veins, and intervertebral disks (Table 1).

We used the anatomical and segmented images of the VKH from kidneys to testes. The VKH of the entire body included 8,590 anatomical images with 0.2 mm intervals (Park et al., 2005a). Among them, we selected the images from top of the left kidney to bottom of the testes; as a result, 2,200 images (numbers, 2,601 to 4,800) of anatom-

ical images were prepared. Successively, we selected every five slice; as a result, 440 images (numbers: 2,605, 2,610, 2,615, . . . 4,800) of anatomical and segmented images with 1 mm intervals were prepared (Fig. 2).

Segmentation and 3D reconstruction of the urogenital tract were performed using the SURFdriver software (PC version 3.56) in the environment of Windows 2000 NT of the personal computer (CPU, 3 GHz; RAM, 512 KBytes; HD, 60 GBytes) at Paris 5 University (Ameil et al., 1984; Lozanoff and Diewert, 1989a, 1989b; Moody and Lozanoff, 1997).

General Purpose

First, we used 440 segmented images provided with the VKH. They include the outline of kidneys, urinary bladder (outer boundary), abdominal aorta, renal arteries, lumbar vertebrae, sacrum, hip bones, femurs, and skin. The segmented images were brought to the SURFdriver software version 3.56 (Table 1).

In order to complete segmentation of the images, additional anatomical structures were also segmented. These included the ureters, urinary bladder (inner boundary), urethra, testes, epididymides, ducti deferens, seminal vesicles, prostate, rectum, anal canal, superior mesenteric artery, inferior vena cava, renal veins, and intervertebral disks (Table 1). This task was accomplished using the SURFdriver software.

Main Steps and Functions of Software

Creation of new 3D objects. Each 3D object representing an anatomical structure was built separately, identified by placing chains of vertices around the object edges, referred to as "contours." Each distinct area of the object within the image was mapped with a separate contour. A variety of tools facilitated the placement of contours, including the Autocontour tool, which selects areas of similar color and places vertices automatically around the object edge using a user-specified density. Figure 4 shows the software interface.

Scale measurement. The scale parameters were entered on the image plan (field of view, 600 mm × 400 mm) in order to make possible distance and volume calculations.

Edition of contours of created objects. Once created, an object's contour could be edited and modified for each slice with the available tools located on the left upper side of the screen (Fig. 4). Each control point of the contour can be erased or moved. Another point can be added.

Creation of 3D objects from contours (surfacing of objects). Intersection planes between contours and volumes were identified and surface tiles were carved from these intersections. Tiles were depth-sorted and the associated surface was rendered (Lozanoff and Diewert, 1989a; Lozanoff and Deptuch, 1991).

Once the contours had been assigned to each serial image containing the object, vertices were connected using a surfacing routine developed especially for SURFdriver software. This routine computes and refines a best-fit solution for assembling the vertices into a volumetrically optimized solid.

Viewing 3D model. Three-dimensional model could be displayed, rotated, or zoomed with the SURFdriver software. Any combinations of the anatomical objects
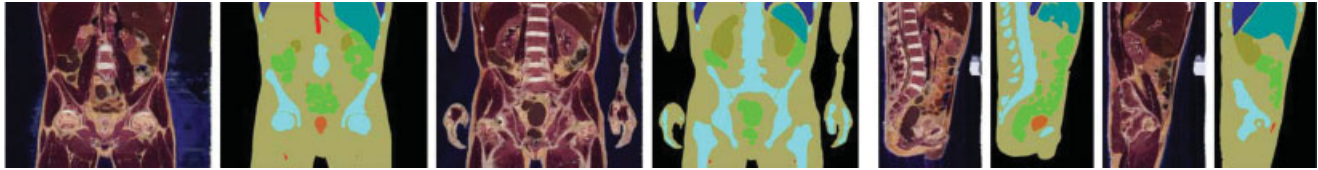
Fig. 3. Coronal and sagittal planes of the anatomical and segmented images of the VKH from kidneys to testes.

TABLE 1. Urogenital tract and adjacent anatomical structures, which are segmented and 3D reconstructed as 42 different anatomical objects

Systems	Anatomical structures (Actual numbers of structures)
Urinary	Kidneys (2), Ureters (2)*, Outer boundary of urinary bladder (1), Inner boundary of urinary bladder (1)*, Urethra (1)*
Genital	Testes (2)*, Epididymides (2)*, Ducti deferens (2)*, Seminal vesicles (2)*, Prostate (1)*
Digestive	Rectum (1)*, Anal canal (1)*
Vascular	Abdominal, aorta (1), Superior mesenteric artery (1)*, Renal arteries (2), Inferior vena cava (1)*, Renal veins (2)*
Skeletal and Articular	Lumbar vertebrae (5), Intervertebral discs (6)*, Sacrum (1), Hip bones (2), Femurs (2)
Integumentary	Skin (1)

*The anatomical structures are segmented on the SURFdriver software while the remaining ones are segmented on the Adobe Photoshop software version 7.
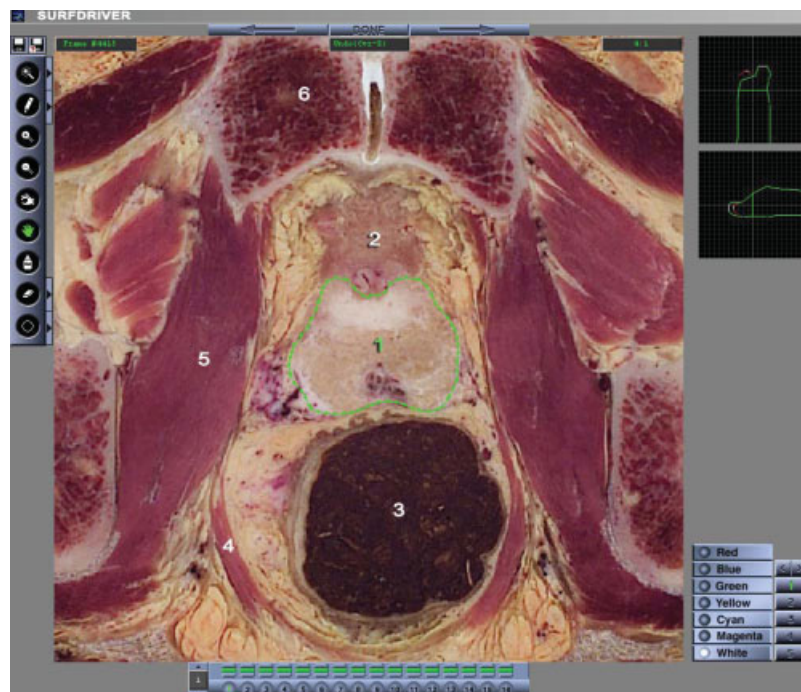

Fig. 4. Interface screen of the SURFdriver software (version 3.5) for drawing of the boundaries of the prostate (green line and points) on the image number 4,415. On the left, working tools. Right windows the 3D object being constructed in the coronal and sagittal planes. 1, prostate; 2, urinary bladder; 3, rectum; 4, levator ani; 5, medial obturator muscle; 6, pubic bone.

could be selected for display. Any 3D object could be textured and displayed with a transparency rate from 0 to 100%. The 3D model could be magnified, moved, and rotated at free angles. On a personal computer, the 3D model could be displayed and rotated in real time because the 3D model was made by surface reconstruction.

Export of 3D model. Once created and surfaced, the model could be exported to be processed with another 3D or CAD software. The export formats available are dxf, Iges 1 to 3.

Additional features. An additional feature of the viewer was the ability to smooth objects or reduce the surface angularities caused by aberrant vertices using a modified shortest path algorithm. This resulted in cleaner surface definition and better rendering. The surfaces of each anatomical structure's 3D model were
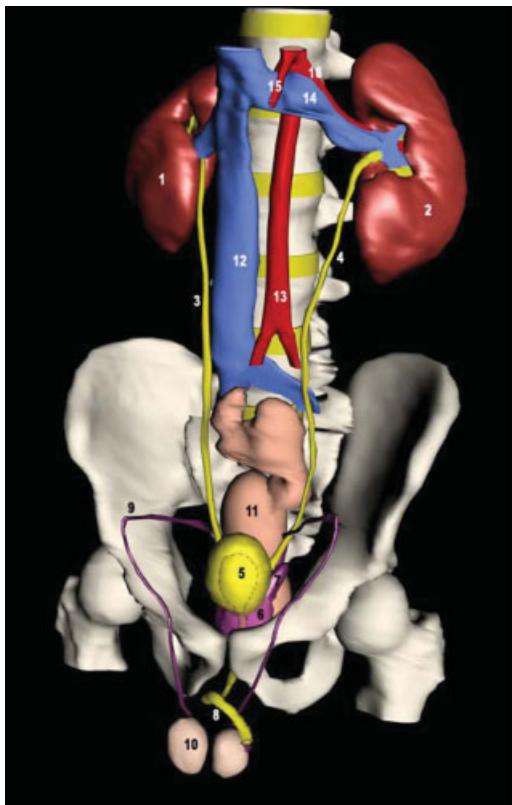
Fig. 5. Three-dimensional images of the urogenital tract and adjacent anatomical structures, which are displayed opaquely with exception of the semitransparent urinary bladder and prostate. 1, right kidney; 2, left kidney; 3, right ureter; 4, left ureter; 5, urinary bladder (inner and outer boundaries); 6, prostate; 7, left seminal vesicle; 8, urethra; 9, right ductus deferens; 10, right testis; 11, rectum; 12, inferior vena cava; 13, abdominal aorta; 14, left renal vein; 15, superior mesenteric artery; 16, left renal artery.

Fig. 6. Three-dimensional model of the urogenital tract with bones after removal of the other anatomical structures.

colored, and texture was applied to obtain a more realistic result.

A special display mode, which yielded shadows of the 3D model, was available to provide a stereoscopic effect by using red and green glasses.

RESULTS

The final result, available as an interactive 3D model on a PC monitor, is shown in Figures 5–10. Figure 5 shows the overall aspect of whole anatomical structures displayed as 3D objects together. Figure 6 represents the urogenital tract with the bones after removal of the other anatomical structures. On Figure 7, the urogenital tract with the bones is rotated; the urinary bladder's inner boundary and prostatic urethra are visible thanks to the semitransparent urinary bladder and prostate.

Figure 8 shows a zoomed view of the pelvis, in which anatomical structures were definite without pixels limitation. In Figure 9, the same with the removal of left hip bone was shown. Figure 10 represents an overall lateral view with a semitransparent skin.

In summary, the interactive 3D model of 42 anatomical structures could be displayed with the following functions. Any combination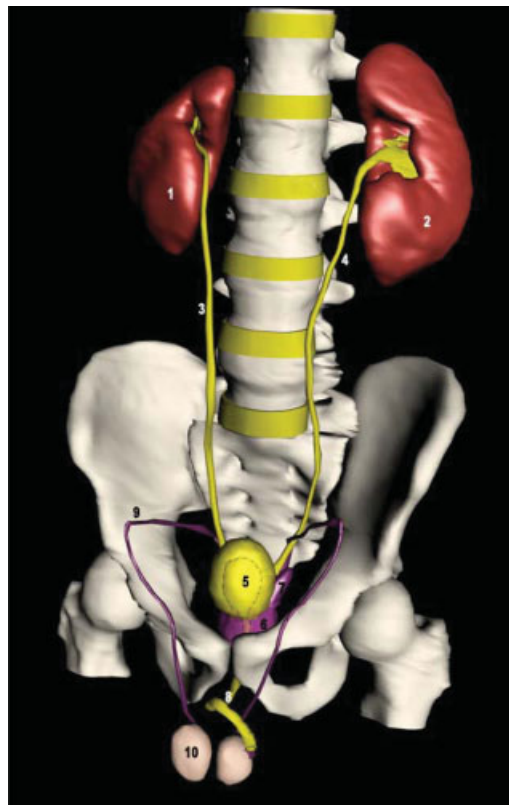s of the anatomical 3D model could be selected for display. The 3D model was appropriately shaded for stereoscopic effect. Some 3D model could be made semitransparent. The 3D model could be zoomed in or zoomed out without pixels limitation. The 3D model could be rotated at free angles (Figs. 5–10). An interactive display is possible in real time on a personal computer.

The 3D model scale proportion was verified by comparing the superior-inferior scale with the anterior-posterior position and bilateral scales (Figs. 5–10). This result was obtained by the careful intervals adjustment of stacked segmented images.

DISCUSSION
Comments About Our Results

All 3D images made in this research will be presented worldwide free of charge either online or offline. The interactive 3D model is expected to help medical students for the study of anatomy. In addition, the 3D model is expected to help medical doctors explain urological diseases to patients (Figs. 5–10).

On the basis of the 3D images presented in this research, other educational software is expected to be composed. This application is easy to use especially because surfaced objects are rendered in the SURFdriver viewing window. Multiple objects created using the same image files can be loaded concurrently, and SURFdriver automatically places objects in the correct alignment with one another. Objects in the viewer can be exported using two popular 3D file formats, DXF and IGES, which are both
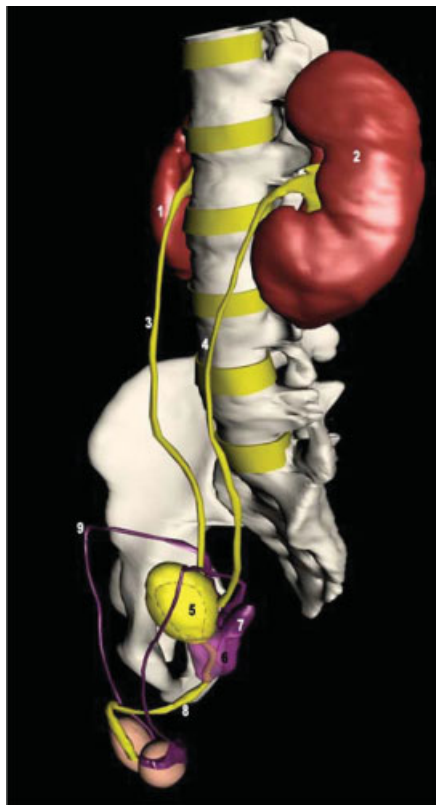
Fig. 7. Rotated 3D model of the urogenital tract with bones. The urinary bladder's inner boundary and prostatic urethra are visible thanks to the semitransparent urinary bladder prostate.
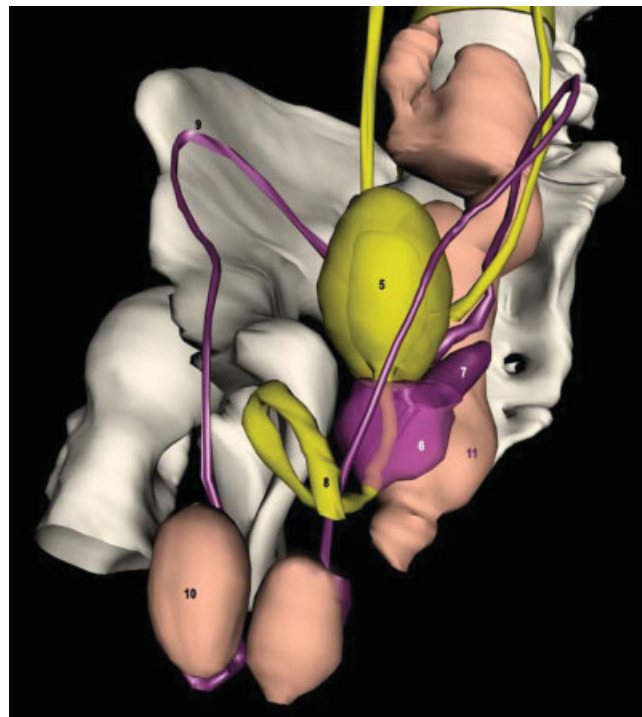

Fig. 8. Zoomed 3D model of the pelvis.

Fig. 9. Three-dimensional model of the pelvis after removal of the left iliac bone.
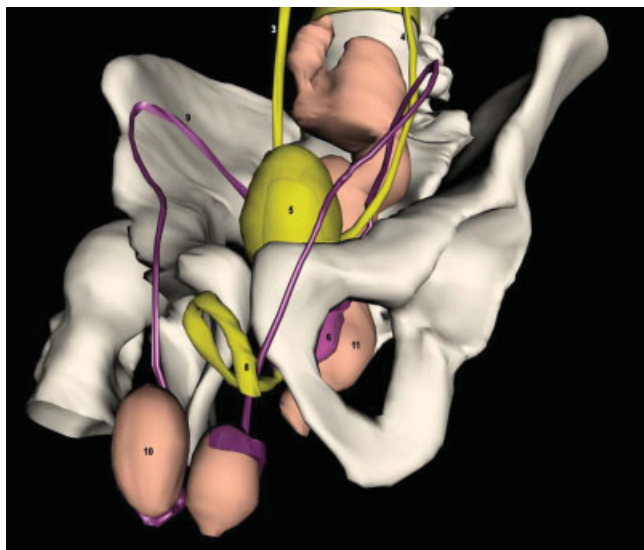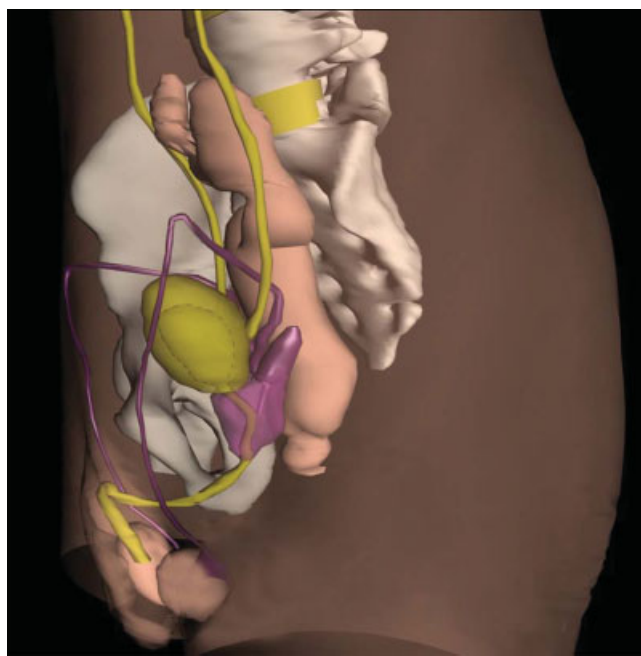

Fig. 10. Lateral view of 3D model of the pelvis with skin's semitransparency.

used by a variety of CAD and 3D software rendering packages. In addition, a simple way to display the 3D images is to use the software from Apple (Nieder et al., 2000) QuickTime virtual reality.

A set of 36 images of a rotation of 360° is loaded in the horizontal layers of QuickTime (one image every 10°). Each layer represents different transparencies of the anatomical structures. Using this method allows interactive

manipulation of the 3D model on a personal computer in real time. This is accomplished by moving the mouse horizontally, and the model rotates on its vertical axis; by moving the mouse vertically, the transparency of the anatomical structures is modified.

The efficiency of this 3D modeling tool to learn anatomy and as surgical simulators has been successful for teaching students (Pugh et al., 2001) as well for patients before operations (Hermann, 2002). Also, it has been compared to other tools and is of better educational value thanks to the direct manipulation of segmented 3D graphical models by the user (Kim et al., 1999)

Possible Improvements of Our Research

For enhancing the educational power of the 3D images, several improvements are to be achieved.

First, additional anatomical structures need to be segmented. For example, the urogenital system-related muscles such as the pelvic diaphragm and perineal muscles need to be included. In addition, some anatomical structures need to be segmented in detail. For example, the renal cortex, renal pyramids, minor calices, major calices, and renal pelvis in a kidney need to be further segmented. If the segmentation is performed on the anatomical images with 0.2 mm-sized intervals and pixels, it is possible to make elaborate 3D model of the tiny anatomical structures such as bulbourethral glands.

Second, 3D models need to be made by solid modeling. The 3D model of the anatomical structures made by solid modeling can be sectioned at free angles to display sectional planes. On the sectioned planes, we cannot only see anatomical images with real body colors but also computed tomographs or magnetic resonance images, both of which correspond to the anatomical images included in the whole VKH data (Park et al., 2005a). Another trial is the use of a 3D model made by solid modeling (Boissonnat, 1988).

Third, virtual dissection with various functions needs to be tried. For example, if the mouse pointer is put on an anatomical structure of the 3D model, the name of the anatomical structure is displayed. For this trial, it is necessary not only to investigate other virtual dissection software but also to listen to the opinions of many health science students and medical doctors (Schiemann et al., 2002).

Fourth, virtual surgery needs to be implemented. For example, virtual transurethral prostatectomy needs to be tried to improve the skill of the urologist. It is more desirable to make the virtual transurethral prostatectomy system including computer, transurethral endoscope equipped with haptic device, and mannequin, all of which are interactively linked.

In fact, advanced simulator training within medicine is a rapidly growing field. Virtual reality simulators are being introduced as powerful and cost-saving educational tools, which also lead to increased patient safety. In this respect, several surgical simulators have been evaluated for their learning capabilities. An E-pelvis simulator has been evaluated by Pugh et al. (2001). The SISILAP-G for training minimal invasive interventions was used in gynecology (Radetzky et al., 1999). Validation and learning were assessed by the Procedicus KSA virtual reality surgical simulator for endoscopy (Strom et al., 2003).

Fifth, 3D model needs to be movable. For example, according to urinary flow, 3D models of the urinary bladder should become expanded or shrunken with urinary flow. This would fulfill not only anatomical demand but also physiological demand.

Sixth, 3D model of female pelvic anatomy needs to be used as a learning tool. Therefore, in the near future, VKH has a plan to section a female cadaver serially to create high-quality anatomical and segmented images of the female.

LITERATURE CITED

Ameil M, Delattre JF, Cordobes B, Flament JB. 1984. Computerized reconstruction of an anatomical structure based on digitized sections: preliminary study. Anat Clin 5:261–264.

Boissonnat JD. 1988. Shape reconstruction from planar cross sections. Comput Vis Graph Image Proc 44:1–29.

Brooks JD, Chao W, Kerr J. 1998. Male pelvic anatomy reconstructed from the visible human data set. J Urology 159:868–872.

Hermann M. 2002. 3-dimensional computer animation: a new medium for supporting patient education before surgery—acceptance and assessment of patients based on a prospective randomized study, picture versus text. Chirurgery 73:500–507.

Juanes JA, Prats A, Lagandara ML, Riesco JM. 2003. Application of the Visible Human Project in the field of anatomy. Eur J Anat 3:147–159.

Kim S, Brinkley JF, Rosse C. 1999. Design features of on-line anatomy information resources: a comparison with the Digital Anatomist. Proc AMIA Symp. p 560–564.

Lozanoff S, Diewert VM. 1989a. A computer graphics program for measuring two- and three-dimensional form change in developing craniofacial cartilages using finite-element methods. Comput Biomed Res 22:63–82.

Lozanoff S, Diewert VM. 1989b. Developmental morphology of the Solum Nasi in the mouse lemure (*Microcebus murinus*). J Morphol 202:409–424.

Lozanoff S, Deptuch J. 1991. Implementing Boissonnat's approach for generating surface models of craniofacial cartilages. Anat Rec 229:556–564.

Moody D, Lozanoff S. 1997. SURFdriver: a practical computer program for generating three-dimensional models of anatomical structures. Honolulu, Hawaii: 14th Annual Meeting of the American Association of Clinical Anatomists.

Nieder GL, Scott JN, Anderson MD. 2000. Using QuickTime virtual reality objects in computer-assisted instruction of gross anatomy: Yorick. VR Skull Clin Anat 13:287–293.

Park JS, Chung MS, Hwang SB, Lee YS, Har DH, Park HS. 2005a. Visible Korean Human: improved serially sectioned images of the entire body. IEEE Trans Med Imaging 24:352–360.

Park JS, Chung MS, Hwang SB, Lee YS, Har DH. 2005b. Technical report on semiautomatic segmentation using the Adobe Photoshop. J Digit Imaging 18:333–343.

Pugh CM, Srivastava S, Shavelson R, Walker D, et al. 2001. The effect of simulator use on learning and self-assessment: the case of Stanford University's E-Pelvis simulator. Stud Health Technol Inform 81:396–400.

Radetzky A, Bartsch W, Grospietsch G, Pretschner DP. 1999. SUSILAP-G: a surgical simulator for training minimal invasive interventions in gynecology. Zentralbl Gynakol 121:110–116.

Schiemann T, Freudenberg J, Pflesser B, Pommert A, Priesmeyer K, Riemer M, Schubert R, Tiede U, Hähne KH. 2002. Exploring the Visible Human using the VOXEL-MAN framework. Comput Med Imaging Graph 24:127–132.

Spitzer VM, Ackerman MJ, Scherizinger AL, Whitlock DG. 1996. The Visible Human male: a technical report. J Am Med Inform Assoc 3:118–130.

Stephens B, Temkin B, Krummel TM, Heinrichs WL. 2000. Virtual body structures: a 3D structure development tool from visible human data. Stud Health Technol Inform 70:323–326.

Strom P, Kjellin A, Hedman L, Johnson E, Wredmark T, Fellander-Tsai L. 2003. Validation and learning in the Procedicus KSA virtual reality surgical simulator. Surg Endosc 17:227–231.

Venuti JM, Imielinska C, et al. 2004. New views of male pelvic anatomy: role of computer-generated 3D images. Clin Anat 17:261–271.

Zhang SX, Heng PA, Liu ZJ, Tan LW, et al. 2003. Creation of the Chinese Visible Human data set. Anat Rec B New Anat 275:190–195.